JOURNAL OF MATERIALS SCIENCE 7 (1972) 1137–1146

A method for evaluating the time-dependent failure characteristics of brittle materials – and its application to polycrystalline alumina

A. G. EVANS
Materials Department, School of Engineering and Applied Science, University of California, Los Angeles, California, USA

A simple method for evaluating stress intensity factor, crack velocity (K,V) diagrams is described. The method is evaluated for the glass/water system and is shown to generate data that are entirely consistent with data obtained on the same system using other techniques. The method is applied to the alumina/water system and the K,V diagrams are used to predict times to failure (Ψ) and effects of strain-rate on strength (σ_f). The calculated Ψ and σ_f are in excellent agreement with available data.

1. Introduction

It has been established recently [1-5] that the dynamics of crack propagation during stress corrosion (Fig. 1) can be described uniquely by the stress intensity factor (K_I) and the crack velocity (V) for many (and perhaps all) materials. There are up to three regimes of crack growth as K varies from K_0 (at the stress corrosion limit) to K_{IC}. At low K_I, region I, the rate of the chemical reaction (adsorption, diffusion etc.) near the crack tip controls growth; at intermediate K_I, region II, diffusion of the corrosive species to the crack is rate controlling; at large K_I, region III, K_I is close to K_{IC} and there is a mixture of corrosive and mechanical failure.

It has also been shown recently that K,V diagrams can be used successfully to determine any of the time dependent failure properties of a material. For example, time to failure at constant stress [6, 7] and effects of strain-rate (stress-rate) on fracture strength [8] can be predicted with good accuracy. The evaluation of a single K,V diagram thus replaces the many tedious experiments needed to characterize material behaviour in stress corrosive environments. It is important, therefore, to devise simple methods for the rapid and accurate evaluation of K,V diagrams. It is the primary objective of this paper to describe and evaluate such a test.

A number of test techniques have been used previously. For transparent materials it is possible to follow the crack optically [3, 4, 6, 9] to obtain values for both V and K_I at constant

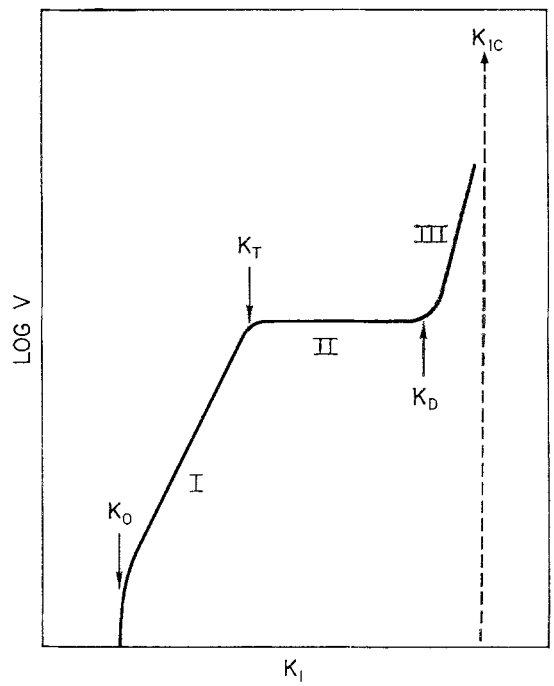

Figure 1 The variation of stress intensity factor, K_I, with crack velocity, V, for a material subjected to a stress corrosive environment.

load. For opaque materials where the crack cannot normally be followed visually, the crack growth rate is usually monitored through a displacement gauge [5] which evaluates the crack opening displacement (COD). The COD is converted into V or K_I through a compliance calibration [5, 10]. The test described in this paper simplifies the experimental procedure very substantially for both opaque and transparent materials. The primary advantages of the test are the elimination of displacement or optical measurements, simple specimen geometries and rapid calibration. The elimination of the displacement measurements has the additional advantage that tests can be conducted in hostile environments or at elevated temperatures without the complexity of remote reading gauges [2]; this is particularly important for very brittle materials, such as ceramics, glass, concrete, etc. where COD values are small and the use of remote gauges introduces substantial inaccuracies. The simple specimen geometries are also of particular importance for very brittle materials, because costly machining operations are minimized.

It is intended in this paper to describe the test technique and to establish the theoretical basis for the evaluation of K, V diagrams. The test is then evaluated in detail for very brittle materials and is shown to be ideally suited to the rapid and accurate determination of K, V relationships. (The application of the technique to less brittle materials will be presented in a subsequent publication.) Finally, the test is used to obtain K, V data for the alumina/water system and hence to predict times to failure and effects of strain-rate on strength.

2. The test technique

The test is based on a technique suggested by Outwater and developed by Kies and Clark [11] (Fig. 2). The specimen is a simple rectangular plate supported on two parallel rollers. The load is applied via two hemispheres attached to the upper plate. The crack propagates along the length of the specimen starting at the end where the load is applied. Usually the specimen is side grooved along the lower face to ensure that the crack propagates along the specimen axis. An analysis by Kies and Clark [11] indicates that K is independent of crack length. This may be confirmed experimentally from a K calibration (Table I). For very brittle materials crack propagation occurs by mode I opening (see Appendix 1) so that:

$$K_I = AP \tag{1}$$

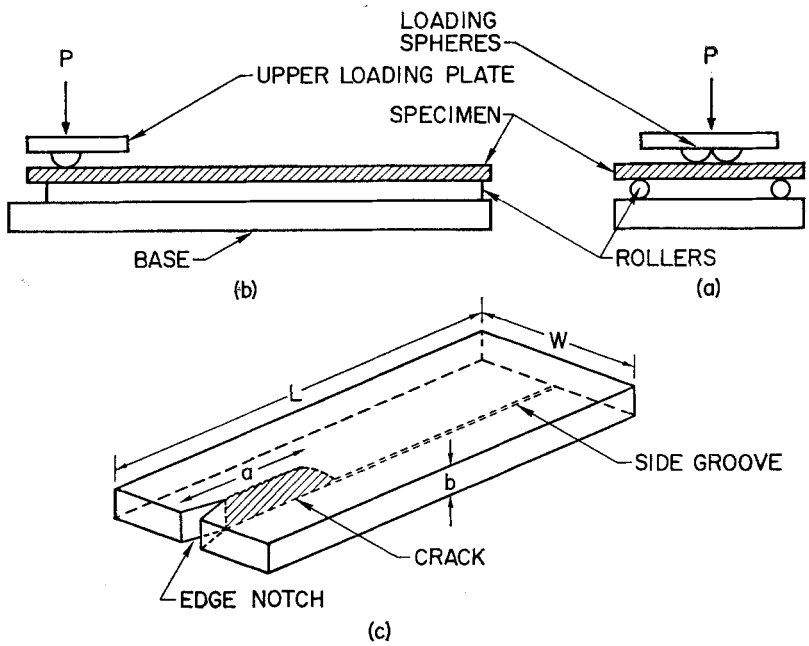

Figure 2 A schematic representation of the test device. (a) Side projection. (b) End projection. (c) The test specimen.

TABLE I K-calibration for a glass specimen

Crack length (cm)	2.0	3.1	4.0	5.2	6.3
Fracture load (kg)	0.92	0.88	0.89	0.90	0.88

where the P is applied load and A is a constant that depends on the dimensions of the specimen and the test device. A compliance calibration (Fig. 3) shows that the displacement of the loading points, y, is linearly related to the crack length, a, and the load, P, so that

$$y = P(Ba + C) \tag{2}$$

where B and C are constants that depend on the elastic modulus of the material and the dimensions of the material and the test device.

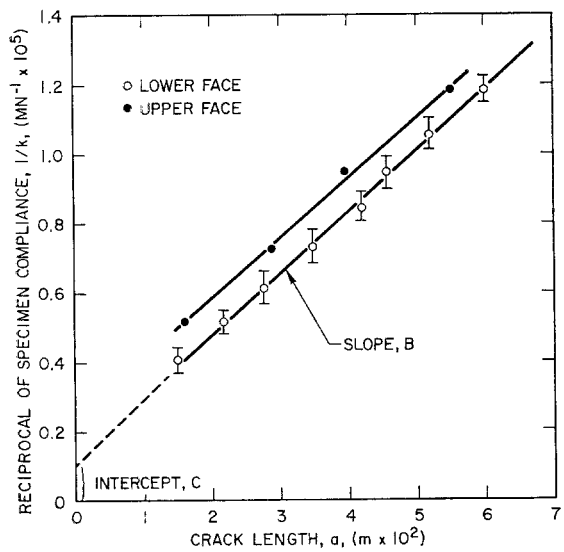

Figure 3 The effect of crack length, a, on the specimen compliance, k. The crack front is inclined to the resultant direction of crack propagation (see Section 3 and Appendix 1) so that different a values are obtained for the lower and upper face for each compliance measurement.

Previously [11, 12] this loading arrangement has been used only as a constant load test with crack velocities evaluated from optical measurements of crack length. Two other approaches are described in the paper which make better use of the unique simplicity of the test technique.

2.1. Load relaxation method

Differentiation of Equation 2 with respect to time (t) gives:

$$\frac{dy}{dt} = (Ba + C)\frac{dP}{dt} + BPV \tag{3}$$

Thus, at constant displacement, $(dy/dt = 0)$

$$V = -\frac{(Ba + C)}{BP}\frac{dP}{dt} \tag{4}$$

Also, at constant displacement,

$$P(Ba + C) = P_i(Ba_i + C) \tag{5}$$

where a_i is the crack length and P_i is the load at the onset of relaxation.

Substituting for a in Equation 9 gives:

$$V = -\frac{P_i}{P^2}\left[a_i + \frac{C}{B}\right]\left(\frac{dP}{dt}\right) \tag{6}$$

For large a_i this reduces to

$$V = -\frac{a_i P_i}{P^2}\left(\frac{dP}{dt}\right). \tag{7}$$

The crack velocity can thus be obtained directly from the rate of load relaxation at constant displacement and the initial crack length. The relaxation experiment can be conducted very simply in a constant crosshead displacement machine, such as an Instron. The initial crack length a_i is measured and a predetermined load P_i is applied, at a high crosshead displacement rate so that no significant crack extension occurs prior to the relaxation. When P_i is reached the crosshead is arrested and the load relaxation is followed on the recorder. In this way a wide range of crack velocities ($> 10^{10}$ m sec^{-1}) may be obtained on the same specimen.

The corresponding values of K_I are found directly from the load P (for each dP/dt) via Equation 1. An analytical value for A is available [11] but a more satisfactory value may be determined empirically for each specimen as follows. When relaxation is complete, the crack is propagated to failure at a high crosshead displacement rate (preferably in the absence of the corrosive environment) where fracture is entirely mechanical, i.e. $K_I = K_{IC}$. Since K_{IC} for the material can be determined very precisely using a variety of independent techniques A may be determined with good accuracy from the crack extension load, P_{IC}.

The entire K, V diagram is thus obtained on a single specimen from measurements of the load/time relationship at constant displacement, the initial crack length and the load for rapid crack propagation*.

*If relatively small intial crack lengths a_i, need to be used, values for B and C are also required to evaluate V. These may be obtained from measurements of the specimen compliance both prior to relaxation (where $a = a_i$) and after relaxation.

2.2. Incremental method

Another method for obtaining information about K, V diagrams, which may be regarded as complementary to the relaxation method, entails incremental changes in displacement rate or temperature at constant crack length. The resultant load increments give accurate values for the slopes of the K, V curve and the activation enthalpy (ΔH) respectively.

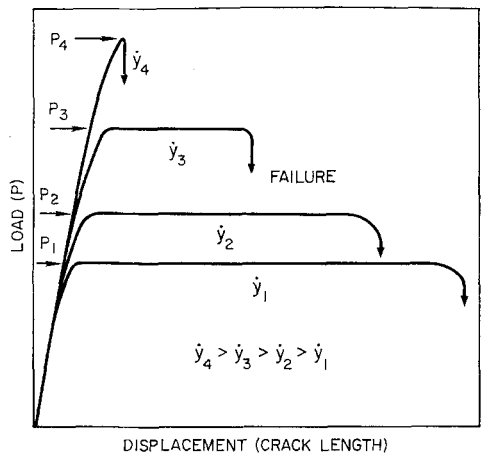

Figure 4 Effect of displacement rate, $\dot{y}$, on the load, deflection curve, in regions I or III.

At constant displacement rate, $\dot{y}$, it is found that the crack propagates at constant load (Fig. 4); from Equations 1 and 3 therefore,

$$\dot{y} = BPV = \frac{B}{A} K_I V \tag{8}$$

K_I and V are related by [3, 13]

$$V = \alpha \exp\left(-\frac{\Delta H}{RT}\right) \exp\left(\frac{\lambda K_I}{RT}\right) \tag{9a}$$

where λ is an activation volume, α is a constant, T is the temperature and R is Boltzmann's constant, or, [8, 14]

$$V = \alpha' \exp\left(-\frac{\Delta H}{RT}\right) K^n \tag{9b}$$

where α' is a constant. Most data can be fitted to either relationship [8]. Consider for convenience Equation 9b. At constant temperature, substituting V from Equation 9b into Equation 8 gives:

$$\dot{y} \propto K_I^{n+1}$$

For a change in displacement rate from $\dot{y}_1$ to $\dot{y}_2$ therefore:

$$\dot{y}_1/\dot{y}_2 = (K_1/K_2)^{n+1} = (P_1/P_2)^{n+1}$$

or,

$$n = \log(\dot{y}_1/\dot{y}_2)/\log(P_1/P_2) - 1 \tag{10}$$

The load increment gives directly a value for the slope n of the K, V curve at each K_I. Since the experiment is conducted at constant crack length, and hence at constant microstructure, n is determined very accurately. This n may be used in conjunction with the relaxation data to construct accurate K, V diagrams.

For a change in temperature from T_1 to T_2 at constant $\dot{y}$ Equations 8 and 9b give:

$$P_1^{n+1} \exp\left(-\frac{\Delta H}{RT_1}\right) = P_2^{n+1} \exp\left(-\frac{\Delta H}{RT_2}\right) \tag{11}$$

where n and ΔH are generally found to be temperature independent [6]. The activation enthalpy is given by:

$$\Delta H = \frac{RT_2T_1}{(T_2 - T_1)} (n + 1) \ln\left(\frac{P_1}{P_2}\right) \tag{12}$$

The activation enthalpy is obtained directly from the load increment due to a change in temperature, once n has been determined from an incremental displacement-rate experiment. ΔH can then be used to construct K, V diagrams over a range of temperatures using Equation 9b, or to obtain information about the mechanisms of stress corrosion [15, 16].

3. Experimental controls

The accuracy of the incremental method is not significantly affected by the experimental conditions and no special precautions are needed to obtain good data.

The effective use of this relaxation method is, however, dependent on certain experimental requirements; related primarily to the elimination of extraneous relaxations. There are two principal sources of extraneous relaxation, thermal and plastic. Thermal instability leads to the expansion (or contraction) of the test material and test device, resulting in load variations at constant displacement. Accurate data can only be obtained therefore when the test system is in thermal equilibrium. Plastic relaxation may occur in materials which exhibit extensive plastic flow, i.e. some metals and polymers. If plastic relaxation cannot be entirely eliminated, it is often possible to obtain good crack-propagation data by analysing the relaxation on an unnotched specimen [17].

Observations of the crack front at various stages during propagation (Fig. 5) show that the

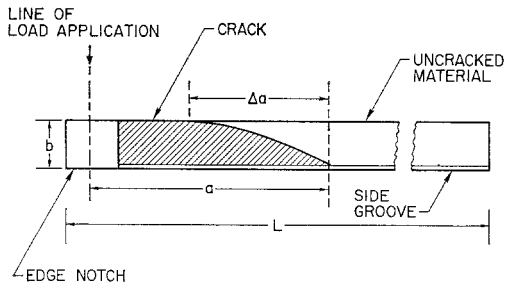

Figure 5 The crack front in the test specimen, showing that the crack extends further along the lower face.

crack extends further along the lower face than the upper face by an amount Δa^*. For glass and alumina the ratio $\Delta a/b$ is ~ 5, independent of the crack length (except for very short cracks). The velocity of the crack front is not therefore given directly by da/dt as assumed in the analysis in Section 2.1; it is smaller by an amount determined by the ratio $\Delta a/b$, Thus, Equation 7 becomes:

$$V = -\phi \frac{a_i P_i}{P^2} \left(\frac{dP}{dt}\right) \quad (13)$$

where $\phi = b/\sqrt{(\Delta a^2 + b^2)}$. Observations of the crack profile are needed therefore to obtain accurate velocity data.

4. Method verification

The ultimate value of these methods for evaluating K, V diagrams is determined by the reliability of the data generated. It is essential, therefore, that the data is compared with data obtained using other techniques. K, V diagrams for the glass/water system are probably the best documented [3, 6, 15] and the most reproducible since microstructural variations are minimal. Data for the soda-lime glass/distilled water system is thus obtained using these methods and compared with the available data on the same system.

4.1. Incremental method

4.1.1. Increments in displacement rate

Order of magnitude increments are found to give satisfactory increments in load. For $\dot{y} = 2$ cm min^{-1} fracture is entirely mechanical; values of n can therefore be evaluated for $\dot{y}$ between 0.005 cm min^{-1} (the lowest value for the available Instron) and 2 cm min^{-1}. The results are presented in Table II; n is found to be 14.1 independent of K_I.

TABLE II Incremental displacement-rate experiments to evaluate n

$\dot{y}_1$ (cm min^{-1})	$\dot{y}_2$ (cm min^{-1})	P_1 (kg)	P_2 (kg)	n
0.005	0.05	0.655	0.765	14.2
0.05	0.5	0.750	0.875	14.0
0.005	0.5	0.640	0.870	14.1
0.5	2.0	0.860	0.950	14.0
0.05	2.0	0.745	0.955	14.2

4.1.2. Increments in temperature

Increments in temperature of 30°C give satisfactory increments in load. Values of ΔH are obtained between 25 and 85°C for various $\dot{y}$. The results are presented in Table III. ΔH is found to be 23.2 ± 0.3 kcal/mol, independent of temperature and independent of K within the ranges considered. This compares with a value of 26 ± 1 kcal/mol obtained by Wiederhorn for a similar system [15, 13].

4.2. Relaxation method

The load is applied to a precracked specimen, at $\dot{y} = 2$ cm min^{-1}, to $P \sim 0.95 P_{IC}$, the crosshead is then arrested and the load allowed to relax. A large number of separate tests have been conducted, and data from three of these are shown in Fig. 6 (the value used for K_{IC} is that obtained by Wiederhorn [22]), the upper and lower sets of data are the extreme values for this series. The results are consistent for a wide range

TABLE III Incremental temperature experiments to evaluate ΔH

$\dot{y}$ (cm min^{-1})	T_1 (°C)	T_2 (°C)	P_1 (kg)	P_2 (kg)	ΔH (kcal mol^{-1})
0.005	25	55	0.650	0.515	23.0
0.005	55	85	0.525	0.435	23.5
0.05	25	55	0.720	0.560	24.0
0.05	55	85	0.540	0.450	23.5
0.5	25	55	0.850	0.605	23.0

*See Appendix 1.

of a_i from $a_i/b = 10$ (the smallest value used) up to $a_i/b = 50$ (for $a_i/b > 50$ the crack is close to the end of the specimen and crack propagation can occur rapidly, leading to erroneously large values for V). The slope, n, of the K, V curves is found to be constant for $K \geqslant 2.0 \times 10^5$N $m^{-1/2}$, and can be fitted without much deviation to the slope found from the incremental tests ($n = 14.1$), as shown for the upper set of data in Fig. 6. For $K < 2.0 \times 10^5$N $m^{-3/2}$, n increases and there appear to be a stress corrosion limit, K_0 at $\sim 1.75 \times 10^5$N $m^{-3/2}$.

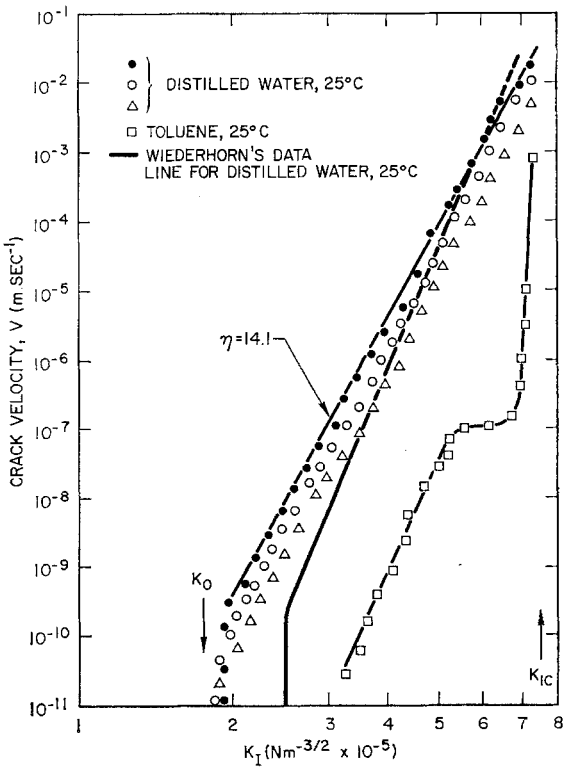

Figure 6 Crack velocity, stress-intensity factor data obtained for the soda-lime glass/water system at 25°C using the relaxation technique. The line drawn through the upper set of data corresponds to the slope obtained using the incremental method. The data are compared with data obtained by Wiederhorn [6] on a similar system.

Included on the graph in Fig. 6 is the data line for Wiederhorn's tests on a similar system [6]. Apart from a small difference in slope (Wiederhorn's data give $n = 16$) and in K_0 the agreement is very good. The differences in n and K_0 are within the variations that can be obtained due to differences in glass composition [6] and water purity.* The excellence of the correlation for both K, V and ΔH shows that this technique, used in the ways described here, can generate data with good accuracy at least for materials which do not exhibit plastic relaxation during testing.

Finally, to demonstrate that the correlation for tests in water was not fortuitous, some tests were carried out in toluene which has a very low residual water concentration. The data is shown in Fig. 6. This curve is identical to those obtained by Wiederhorn [3] for crack propagation in environments containing small concentrations of water. The test therefore gives an accurate measure of the effect of water concentration on the K, V curve, thereby providing additional qualitative verification of the test method.

5. Stress corrosion in the alumina/water system

Although data are available for sub-critical crack extension in single crystals of alumina [4] (where transparency allows optical methods to be used for evaluating crack velocities) there are no data for polycrystalline alumina. There is substantial experimental evidence that polycrystalline alumina exhibits stress corrosion in water-containing environments [18, 19, 20]. The evaluation of K, V diagrams for this system will thus be of considerable benefit for the prediction of time dependent failure characteristics. Some preliminary data are presented in this section.

5.1. Evaluation of K, V diagram

The tests are conducted on a commercial 95% alumina (hylumina) [18] in moist air (50% humidity) and in toluene. K_{IC} has been determined by Davidge and Tappin [18] at 20°C (in degassed silicone oil), and is 5.3×10^6N $m^{-3/2}$. Incremental displacement-rate experiments give, for region I, $n = 31$. A series of relaxation experiments give the data in Fig. 7: regions I and II and a small region III are apparent. The data for region I fit a slope of 31 with little deviation. This slope is substantially larger than for soda-lime glass but similar to that for single crystals of alumina. Region II occurs at a crack velocity similar to that observed for the glass/water

*Data has subsequently been obtained on the glass/water studied here, using Wiederhorn's technique. The data are in exact correspondence with the relaxation data, verifying that the crack propagation parameters, n and K_0, for this system differ slightly from those for the system studied by Wiederhorn [6].

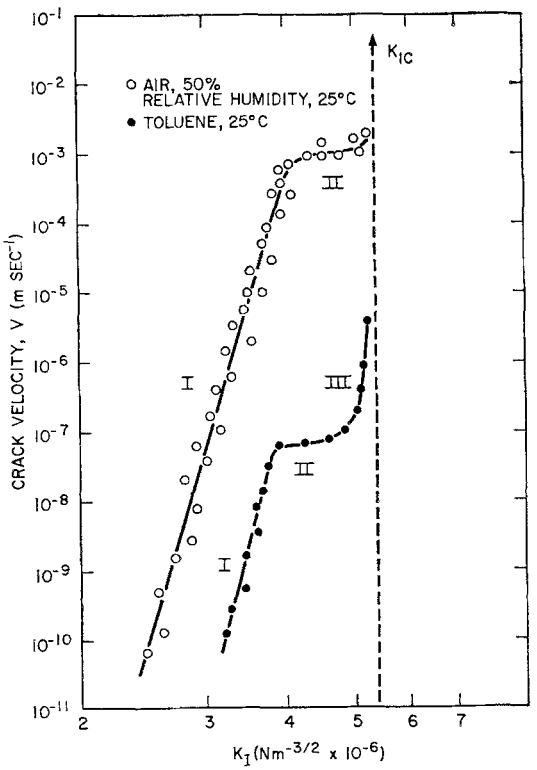

Figure 7 Crack velocity, stress-intensity factor data for polycrystalline alumina in moist air, 50% relative humidity and in toluene. Regions I, II and III are apparent.

system [3, 9] at the same water concentration. This is precisely what is expected since crack propagation in this region is controlled by diffusion in the environment and should be relatively insensitive to the structure of the test material for a given corrosive species. Finally, no stress corrosion limit has been detected for $K > 2.2 \times 10^6$ N m$^{-3/2}$.

5.2. Time-dependent failure characteristics

The K, V diagrams in Fig. 7 can be used to predict times-to-failure (Ψ) and the effects of strain-rate ($\dot{\epsilon}$) on strength (σ_f) for the equivalent environmental conditions.

The time-to-failure at constant stress can be simply evaluated from an integration of the K, V diagram, as follows:

$$\Psi = \int_{a_i}^{a_{IC}} \frac{da}{V} . \qquad (14)$$

The integration is between a_i and a_{IC} because the time to failure for $a > a_{IC}$ is negligible. Also, since

$$K_I = \sigma Y \sqrt{a} \qquad (15)$$

where Y is a geometrical constant [21], Ψ becomes:

$$\Psi = \frac{2}{\sigma^2 Y^2} \int_{K_{I_i}}^{K_{IC}} \frac{K_I}{V} dK_I . \qquad (16)$$

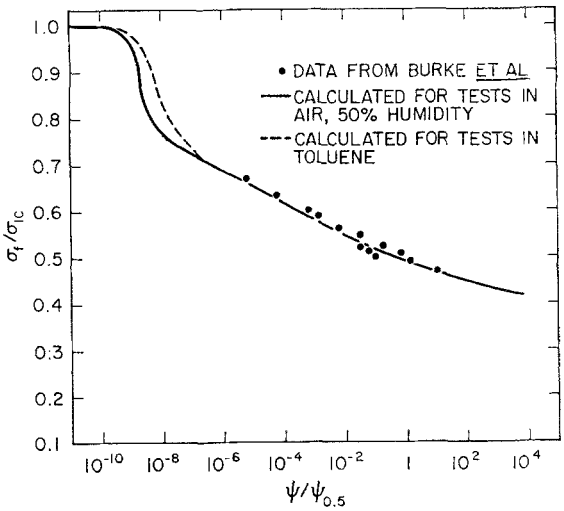

Figure 8 Times to failure for polycrystalline alumina, calculated from the K, V diagram (Fig. 7) and plotted as a universal fatigue curve. $\Psi_{0.5}$ is the time-to-failure at 50% of the stress needed for fracture in an inert environment (σ_{IC}). Also shown are data points obtained on a similar system by Burke *et al* [20].

This integration can be evaluated numerically or analytically. Values of Ψ obtained numerically are shown in Fig. 8, plotted as a universal fatigue curve for easy comparison with available time-to-failure data. The rapidly varying region at small ($\Psi/\Psi_{0.5}$) is due to region II of the K, V diagram, and the less stress sensitive region at larger ($\Psi/\Psi_{0.5}$) is due to region I. Also included in Fig. 8 is time-to-failure data obtained on a similar type of alumina in air at 50% humidity [20]. The data only covers the region of low stress sensitivity, but here the agreement is excellent, thereby providing additional evidence for the validity of both the test method and the use of K, V diagrams for predicting times-to-failure.

The effect of strain-rate on strength can also be obtained from an integration of the K, V curve. An analytical solution to the integration shows that the strength is given, for large n, by [8]:

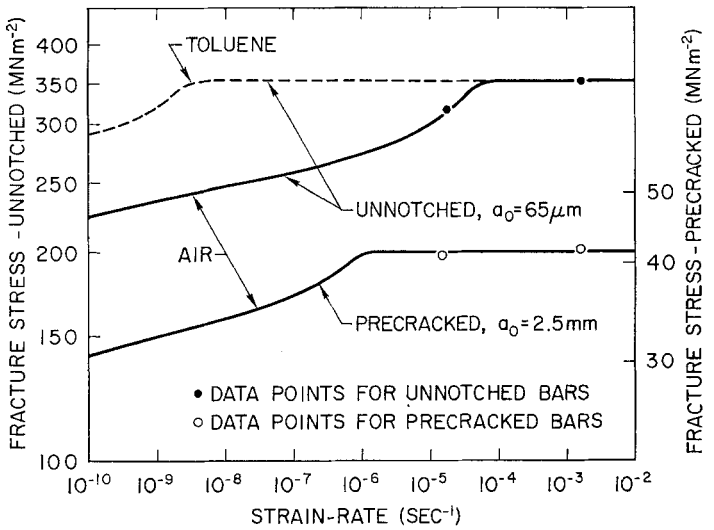

Figure 9 Effects of strain-rate on the strength of polycrystalline alumina calculated from the K, V diagram (Fig. 7). Also shown are data points obtained by Davidge and Tappin [18].

$$\sigma_f = \frac{K_0}{C_0^{1/2} Y_0}\left[1 + \frac{2\pi E \dot{\epsilon}(n+1) a_0^{3/2}}{V_0 K_0 (n-2)}\right]^{1/(n+1)} \left[1 + \frac{\pi E \dot{\epsilon} a_T^{3/2}}{V_T K_T}(a_{IC} - a_T)\right] \quad (17)$$

where $\dot{\epsilon}$ is the applied strain-rate, E is Young's modulus, the subscript 0 refers to conditions at the onset of crack motion and T refers to conditions at the onset of stage II. (A stress corrosion limit K_0 is not apparent in the alumina/water system, but since the variation of crack length with K_I is very small at small K_I [8] – for strain-rates of practical interest – the minimum measured K_I and the corresponding V can be used for K_0 and V_0 without substantially affecting the analysis.) Equation 17 may be used either to construct strength, strain-rate curves for various a_0, or to evaluate a_0 from experimentally determined strengths. Since some strength data is available [18], it is expedient to evaluate a_0 for this material first and then to construct a complete σ_f, $\dot{\epsilon}$ curve. The flexural strength of a 5 × 5 mm specimen tested on a span of 18 mm at a displacement-rate of 0.005 cm min^{-1} (equivalent to a strain-rate in the region of maximum tensile stress of 2.5×10^{-5} sec^{-1}) is 310 MNm$^{-2/3}$. Using these values for σ_f and $\dot{\epsilon}$, a K_I versus crack length diagram can first be constructed [8] to give a_T/a_0 and a_{IC}/a_0. Then a_0 may be evaluated from Equation 17; the analysis gives a_0 = 65 μm and a_{IC} = 80 μm, i.e. an inherent flaw-size equivalent to a through-the-thickness flaw 65 μm deep. From this a_0 a complete σ_f, $\dot{\epsilon}$ curve is constructed as shown in Fig. 9. (Also in Fig. 9 a curve is shown for the effect of strain-rate on the strength of precracked specimens with a_0 = 2.5 mm.) There are very little precise data available to compare with these curves, but where data have been obtained [18] they are entirely consistent with the calculated variations (Fig. 9).

6. Conclusion

A technique for evaluating the variation of stress intensity factor with crack velocity is described. The technique has a number of advantages compared to other available methods. The primary advantages lie in its simplicity and rapidity. It eliminates comprehensive calibration and does not require any crack-opening displacement or optical measurements. In conjunction with these, the simple specimen design gives the additional advantage of low cost.

The design of the test device enables the crack to propagate at constant K_I for a constant applied load. It is shown that at constant displacement, therefore, the rate of load relaxation gives directly the variation of V with K_I. There are no additional requirements for monitoring crack growth.

The accuracy of the method is examined for

the glass/water system by comparing the data with data that has been obtained on a similar system using other techniques. There is a very good correlation showing that the method gives good accuracy, at least for materials that do not exhibit significant plastic relaxation during testing.

The method is applied to the alumina/water system. The K, V diagram generated is used to predict time-to-failure at constant stress and the effects of strain-rate on strength. The predicted variations are in excellent agreement with the available data, giving additional verification of both the test method and the use of K, V diagrams for predicting time dependent failure characteristics.

It is considered, therefore, that the method is ideally suited to the evaluation of the effects of stress corrosion on the time-dependent failure of brittle materials such as glass, ceramics, concrete, rocks, etc. For these materials the analysis is not complicated by plastic relaxation and thin specimens may be used without entering the plane-stress regime. The application of the method to less-brittle materials is currently being studied and will be reported in a subsequent publication.

Acknowledgements

The author wishes to thank Professor A. S. Tetelman and Dr D. P. Williams for very helpful discussions and UKAEA for financial support.

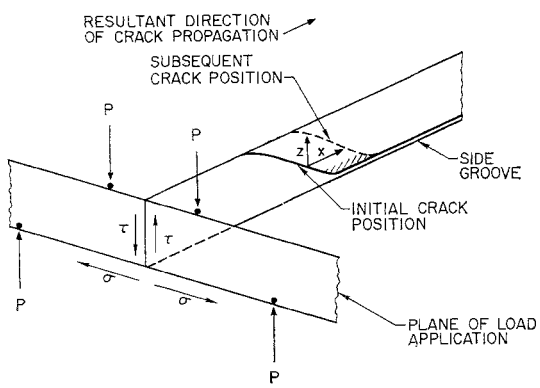

Figure 10 A schematic representation of the relationship between the applied load, P, the stresses generated, σ_t (tensile) and τ (shear), and the crack profile.

Appendix 1

Mode of failure

The resultant direction of crack propagation, x in Fig. 10, suggests that failure occurs due to the shear stresses, τ, i.e. mode III. This would undoubtedly be the operative failure mode if the crack front were parallel to the direction of load application. As shown in Section 3 however, the crack lies closer to the orthogonal direction and the direction of crack propagation is nearly parallel to z. This introduces the possibility that the tensile stresses, σ, due to the applied bending moment may be contributing to the crack growth, so that failure in mode I, or mixed mode I/III occurs. An analysis for K_I and K_{III} is not yet available and it is not possible to predict the failure mode. It is expedient therefore to evaluate G_c* empirically and then to compare this with G_{IC} (and G_{IIIC} when available) for the same material. An empirical G_C determination is conducted here for glass – an example of a brittle material for which $G_{IIIC} \gg G_{IC}$ – using a compliance analysis technique. The compliance calibration is shown in Fig. 3 and the G_C values obtained are listed in Table IV. The measured G_C are in very good agreement with the G_{IC} obtained for soda-lime glass using other techniques (7.6 ± 0.2 J m^{-2}) [22], showing that failure for brittle materials is exclusively mode I.

TABLE IV Compliance analysis for glass to obtain G_c

a (cm)	P_f (kg)	$d(1/k)/da$ ($N^{-1} \times 10^4$)	$G_c = P_f^2\, d(1/k)/d(2ab)$ (J m^{-2})
2.1	0.96	2.0	8.0
3.2	0.92	2.0	7.4
4.0	0.93	2.0	7.5
5.0	0.90	2.0	7.0
5.9	0.92	2.0	7.5

References

1. C. S. CARTER, *Corrosion* **27** (1971) 471.
2. S. MOSTOVOY, H. R. SMITH, R. G. LINGWALL, and E. J. RIPLING, *Eng. Fracture Mech.* **3** (1971) 291.
3. S. M. WIEDERHORN, *J. Amer. Ceram. Soc.* **50** (1967) 407.
4. *Idem, Internat. J. Fracture Mech.* **4** (1968) 171.
5. H. G. NELSON, A. S. TETELMAN, and D. P. WILLIAMS, Proceedings of the International Conference on Corrosion Fatigue, Storrs, Conn., June 1971.

*When failure is exclusively, or even partially, mode I the G_C may only be representative of the material if the side groove is precracked. Then there is no tendency for the leading part of the crack to be impeded (hatched area in Fig. 10) For glass a precrack is introduced very simply using a glass cutter and for ceramics a narrow machined notch is adequate. For more ductile materials it may be necessary to introduce a fatigue crack at the base of the machined side groove.

6. S. M. WIEDERHORN and L. H. BOLZ, *J. Amer. Ceram. Soc.* **53** (1970) 543.
7. D. P. WILLIAMS, to be published.
8. A. G. EVANS, to be published.
9. H. SCHÖNERT, H. UMHAUER, and W. KLEMM, Proceedings of the Second International Conference on Fracture, Brighton 1969, paper 41.
10. D. P. WILLIAMS and H. G. NELSON, *Met. Trans.* **1** (1970) 63.
11. J. A. KIES and A. B. J. CLARK, Proceedings of the Second International Conference on Fracture, Brighton 1969, paper 42.
12. H. R. MCKINNEY and H. L. SMITH, *Bull. Amer. Ceram. Soc.* **50** (1971) 784.
13. S. M. WIEDERHORN, Proceedings of the International Conference on Corrosion Fatigue, Storrs, Conn., June 1971.
14. R. J. CHARLES, *J. Appl. Phys.* **29** (1958) 1657.
15. S. M. WIEDERHORN, N.B.S. Report, 10 444, June 1971.
16. H. G. NELSON, D. P. WILLIAMS, and A. S. TETELMAN, *Met. Trans.* **2** (1971) 953.
17. A. G. EVANS, to be published.
18. R. W. DAVIDGE and G. TAPPIN, *Proc. Brit. Ceram. Soc.* **15** (1970) 47.
19. H. P. KIRCHNER and R. E. WALKER, *Bull. Amer. Ceram. Soc.* **50** (1971) 783.
20. J. E. BURKE, R. H. DOREMUS, A. M. TURKALO, and W. B. HILLIG, G. E. Report No. 71-C-035, Jan. 1971.
21. W. F. BROWN and J. E. SRAWLEY, *ASTM*, STP 410 (1967).
22. S. M. WIEDERHORN, *J. Amer. Ceram. Soc.* **52** (1969) 99.

Received 15 March and accepted 23 March 1972.